V. ELECTRODYNAMICS OF MEDIA*

Academic and Research Staff

Prof. L. J. Chu
Prof. H. A. Haus
Prof. P. W. Hoff
Prof. J. A. Kong
Prof. P. Penfield, Jr.

Graduate Students

M. S. Elkind
D. L. Lyon
E. E. Stark, Jr.

A. ANALYSIS OF TRANSVERSELY EXCITED ATMOSPHERIC (TEA) CO_2 LASER

The TEA CO_2 laser has been of great practical interest to many workers during the last few years,[1-3] but no analysis has yet appeared explaining the dynamics of the laser's operation. In order to unify and explain the experimental data already gathered, we have undertaken such a study. In this report we present the electric field and material rate equations necessary to explain lasing in a mixture of He and CO_2 gases. These equations have been solved numerically by computer, and we compare the results with experiment. We first note several assumptions and numerical values which are peculiar to this laser analysis.

The electric field is represented by a single-frequency component with linear polarization and plane-wave character. Optical losses are lumped into a single cavity Q.

T_2, the relaxation time of the off-diagonal density matrix elements, is predominantly determined by collision processes. Effective cross sections of CO_2 with He and CO_2 have been established experimentally through absorption experiments. Using results of Duscik and Hoag,[4] we have the following total cross section:

$$CO_2\text{-He:} \quad \sigma_{He} = 3.7 \times 10^{-15}\ \text{cm}^2$$

$$CO_2\text{-}CO_2\text{:} \quad \sigma_{CO_2} = 1.3 \times 10^{-14}\ \text{cm}^2.$$

Using the fact that total collision frequency equals the sum of collision frequencies of CO_2 with itself and He, we obtain

$$\frac{1}{T_2} = (1.45 \times 10^4 \sqrt{T}) \left[\sum_{i=He,\,CO_2} N_i \sigma_i \left(\frac{1}{M_{CO_2}} + \frac{1}{M_i} \right)^{1/2} \right],$$

*This work was supported by the Joint Services Electronics Programs (U.S. Army, U.S. Navy, and U.S. Air Force) under Contract DAAB07-71-C-0300, and in part by U.S. Air Force Cambridge Research Laboratories Contract F19628-70-C-0064.

where T = temperature in °K of gas mixture, N_i = density in cm^{-3} of i^{th} gas component, and M_i = atomic weight of a gas molecule of the i^{th} species. Reasonable operating parameters for the TEA CO_2 laser are T = 400°K, partial pressure of He = 300 Torr, of CO_2 = 50 Torr. For these numbers $T_2 = 1.6 \times 10^{-10}$ s, a number which compares favorably with extrapolations from other experiments performed at low pressure.[5] Furthermore, this value is so small that we assume the rate equation limit of the material density matrix equations.

We next assume that the He-CO_2 gas is heated primarily by electron-atom collisions. We assume that most electrical energy is transferred to rotation and/or translation of CO_2 and to translation of He in less than 1 μs after initiation of the discharge.[6] Lasing generally occurs 2.5-3.0 μs after initiation. We draw two conclusions: (i) electrons play an insignificant role in inelastic interactions during lasing, and (ii) the translational temperature of the gas is established at a value which changes only slightly during lasing.

We may roughly estimate the translational temperature rise after discharge by converting the stored electrical energy (0.25 μF at 20 kV) to kinetic motion of the CO_2 and He particles. The resulting value of 400°K for the translational temperature compares well with reported observations.[7] This value is also consistent with the experimental observation that the 10.6 μ P(20) transition is the one most favored by the TEA CO_2 laser.[8]

A set of CO_2, vibrational, basis states is necessary in order to write the rate equations explicitly. In the case of CW laser operation, a single pair of molecular energy eigenstates often proves adequate to explain most phenomena. We have found that a more complete set of states must be used in order to obtain agreement with experimental observations.

In Fig. V-1 we show a selected set of CO_2 energy eigenstates following Herzberg.[9] Higher energy states along the $\alpha 00$ and $0\alpha 0$ modes have been omitted, as well as higher energy combination ($\alpha\beta\gamma$) states. In order to make the preliminary calculation more tractable, a simpler eigenstate scheme is adapted for use.

Figure V-2 shows the eigenstate structure used in the calculation. The asymmetric mode has been made exactly harmonic with spacing = 3365°K. The mode terminates at 00^05. The symmetric stretching mode has been incorporated with the doubly degenerate bending mode because of numerous near-degeneracies (Fermi resonances) encountered in the solution of the zero-order vibrational Schrödinger equation. It has been reasoned that particle-particle collisions are effective in equilibrating Fermi-resonant states in times comparable to T_2.[10]

The resulting symmetric-bend mode is further simplified. The doubly degenerate 01^10 is placed at 960°K. The two 02^20, the 02^00, and the 10^00 are considered strictly degenerate with energy eigenvalue = 1920°K. The two 03^30, the 03^10, and

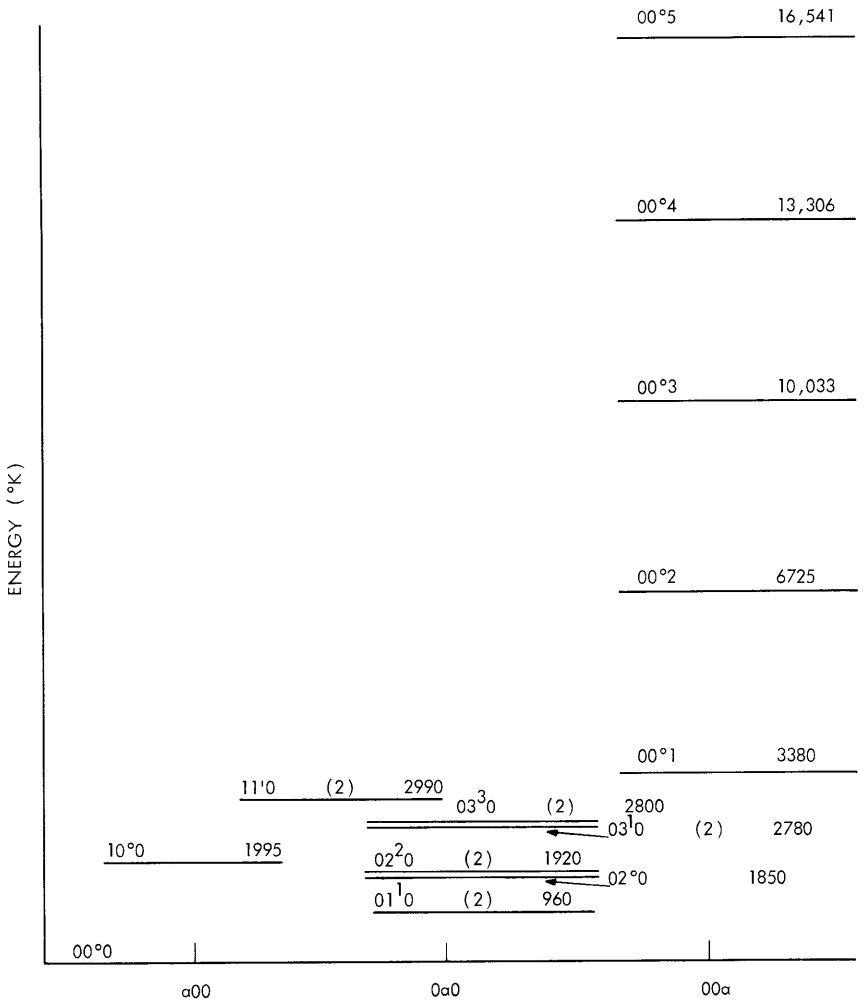

Fig. V-1. Energy eigenvalues for selected CO_2 vibrational levels in the ground electronic state. Degeneracy noted in parentheses.

the two 11^10 states are all considered strictly degenerate with eigenvalue = 2880°K. The higher lying ($\alpha\beta\gamma$) states other than $00^0\alpha$ are represented by equivalent levels coincident in eigenvalues with the 00α's up to 00^05. This is necessary to allow for loss of energy from 00α-$\alpha^1\beta\gamma$ through vibration-vibration type intermode interactions.

With this set of basis functions (represented in Fig. V-2) we may write the rate equations, using the following notation:

$A\alpha$ – refers to 00α, asymmetric mode

$B\gamma$ – refers to the γ^{th} level in the symmetric-bend mode.

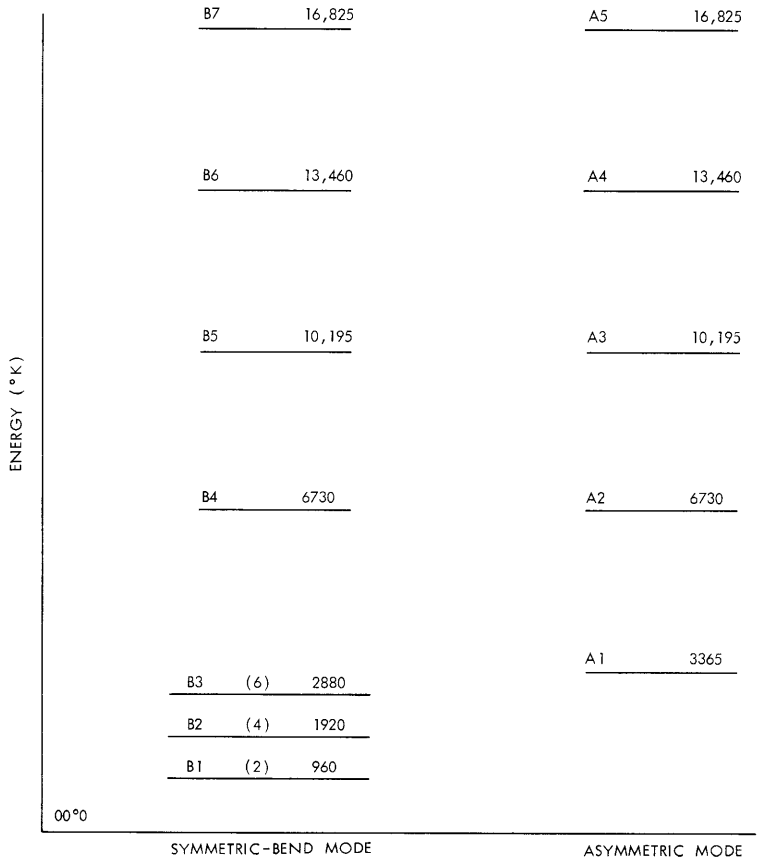

Fig. V-2. Simplified vibrational level structure. Degeneracy noted in parentheses.

The relaxation times associated with each level are determined by collisional processes. In the He-CO_2 system, several different types of collisional interaction occur. CO_2 molecules may exchange internal vibrational energy for translation of helium or other CO_2 molecules (a V-T process). One CO_2 molecule may yield a vibrational quantum of a certain mode while the colliding CO_2 molecule acquires a quantum of the same mode (intramode V-V) or a different mode (intermode V-V).

We make several assumptions in order to describe the effects of the various V-T and V-V processes on vibrational level populations.[11] First, we assume that intramode V-V processes are responsible for establishing a Boltzmann distribution within a particular CO_2 mode while conserving energy in that mode. Furthermore, we assume that intramode V-V processes are much faster than intermode V-V or V-T processes, but possibly no faster than electromagnetic phenomena. Next, we assume that all V-T processes may be lumped together for the symmetric-bend mode and that they are responsible for forcing the vibrational temperature of the mode toward the ambient translational temperature of the gas. We also assume that V-T is relatively ineffective

in relaxing the asymmetric mode. Finally, we assume that intermode V-V processes transfer the energy of the asymmetric mode into the symmetric-bend mode in a time longer than the symmetric-bend V-T time.

With the preceding assumptions, it is possible to define unambiguously time constants associated with the relaxation and/or transfer of total energy in a mode. The time-resolved behavior of any single vibrational level is more complex. For this analysis, we use a set of characteristic times to describe exponential relaxations of individual levels:

TVVA – governs relaxation of populations in asymmetric levels to an MB (Maxwell-Boltzmann) distribution by intramode V-V.

TVVB – governs the same relaxation for the symmetric-bend mode.

TVTA – governs transfer of population from levels in asymmetric mode to symmetric-bend levels resulting from intermode V-V.

TVTB – governs relaxation of symmetric-bend vibrational temperature to the ambient translational temperature.

It is necessary to ascertain dynamically the temperature that intramode V-V tends to establish in the CO_2 modes. In this analysis, these vibrational target temperatures are determined by first finding the values of the total energy in each mode. A calculation is then made which determines the temperatures that would obtain if the two modes were in Boltzmann equilibrium with the energies as found. From this we can calculate equilibrium populations to which intramode V-V drives the levels. The four highest symmetric-bend levels are assumed to have zero equilibrium populations, that is, the symmetric-bend vibrational temperature is assumed always to stay below ~1000°K. Also, we assume that the equilibrium populations to which intermode V-V drives the asymmetric levels are zero. We also assume that the V-T processes act to drive the symmetric-bend mode to a distribution with a temperature equal to 400°K.

Now we may write the 12 independent rate equations governing the vibrational level populations in CO_2. We define:

$$N_i = \frac{\text{Population in } i^{th} \text{ vibrational level}}{(\text{Degeneracy of } i^{th} \text{ level})(\text{Total no. of } CO_2 \text{ molecules})}$$

NE_i = Equilibrium value of i^{th} level population to which intramode V-V drives.

NT_i = Population of i^{th} symmetric-bend level to which V-T drives.

We will not write out the set of equations which determine NE and NT, since in practice these functions are performed by a set of lengthy computer subroutines. We

shall write the set of rate equations.

Lasing levels:

$$\frac{\partial}{\partial t} N_{A1} = -B\epsilon^2(N_{A1}-N_{B2}) - (N_{A1}-NE_{A1})/TVVA - N_{A1}/TVTA$$

$$\frac{\partial}{\partial t} N_{B2} = B\epsilon^2(N_{A1}-N_{B2}) - (N_{B2}-NE_{B2})/TVVB - (N_{B2}-NT_{B2})/TVTB$$

Higher asymmetric levels:

$$\frac{\partial}{\partial t} N_{Aa} = -(N_{Aa}-NE_{Aa})/TVVA - N_{Aa}/TVTA \qquad (a = 2, \ldots 5)$$

Higher symmetric-bend levels:

$$\frac{\partial}{\partial t} N_{B\gamma} = -N_{B\gamma}/TVVB + N_{A(\gamma-2)}/TVTA \qquad (\gamma = 4, \ldots . 7)$$

Remaining symmetric-bend levels:

$$\frac{\partial}{\partial t} N_{B3} = -(N_{B3}-NE_{B3})/TVVB - (N_{B3}-NT_{B3})/TVTB + N_{A1}/TVTA$$

$$\frac{\partial}{\partial t} N_{B1} = -(N_{B1}-NE_{B1})/TVVB - (N_{B1}-NT_{B1})/TVTB,$$

where $B = T_2/\hbar^2 \ |\mu_x|^2 \ D$, $D = 7 \times 10^{-2}$, the fraction of population in J = 19 of 001, and ϵ is the electric field amplitude. The reduced wave equation for the electric field amplitude is

$$\frac{\partial}{\partial t} \epsilon = C(N_{A1}-N_{B2}) \ \epsilon - \frac{\omega}{2Q} \epsilon,$$

where $C = \left(T_2 |\mu_x|^2 \ \omega N_{TOT} \ dD\right)/2\epsilon\hbar L$, and d and L are as indicated in Fig. V-3.

The set of rate equations along with the field equation and the expressions used

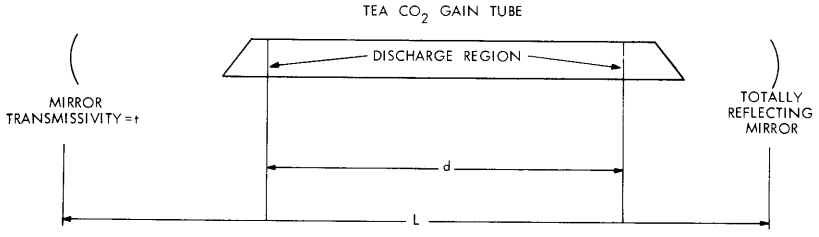

Fig. V-3. Laser schematic.

to find equilibrium level populations must all be solved simultaneously. A set of Fortran IV subprograms has been written to integrate the equations numerically and thus find particular solutions in time for the electric field amplitudes and level populations. The program must be provided with a set of initial conditions for all quantities to be solved, as well as numerical values for all parameters. The following set of values yields a calculated, optical-output intensity which is represented by a dotted line in Fig. V-4.

Initial Conditions:

ϵ = 100 V/m

Asymmetric mode – MB distribution with T = 5000°K

Symmetric-bend mode – MB distribution with T = 400°K.

Parameters (MKS):

$B = 2.7 \times 10^{-6}$ d = 0.9 m

$C = 3.5 \times 10^{8}$ L = 1.8 m

$Q = 1.7 \times 10^{6}$ (which corresponds to losses governed by a 20% transmissivity mirror)

$TVVA = TVVB = 10^{-8}$ s

$TVTA = 2.5 \times 10^{-5}$ s

$TVTB = 5 \times 10^{-7}$ s.

Also plotted in Fig. V-4 (solid line) is the output current from a Ge:Au IR detector which monitored the optical output of a TEA CO_2 laser operating in our laboratory. The laser may be described as follows.

Electrodes – 170 pins (cathode)
170 1 kΩ resistors (anode)

Supply voltage = 19 kV

Capacitance = .025 μF

L = 1.8 m

Mirrors – 4 m radius, 20% transmissivity
10 m radius, Gold

Total gas pressure = 350 Torr

P_{He} = 300 Torr P_{CO_2} = 50 Torr

Total flow = 2 atm-liter/min.

The two curves in Fig. V-4 have been normalized so that each has the same peak power. Time-integrated power (energy) of individual optical pulses has been determined

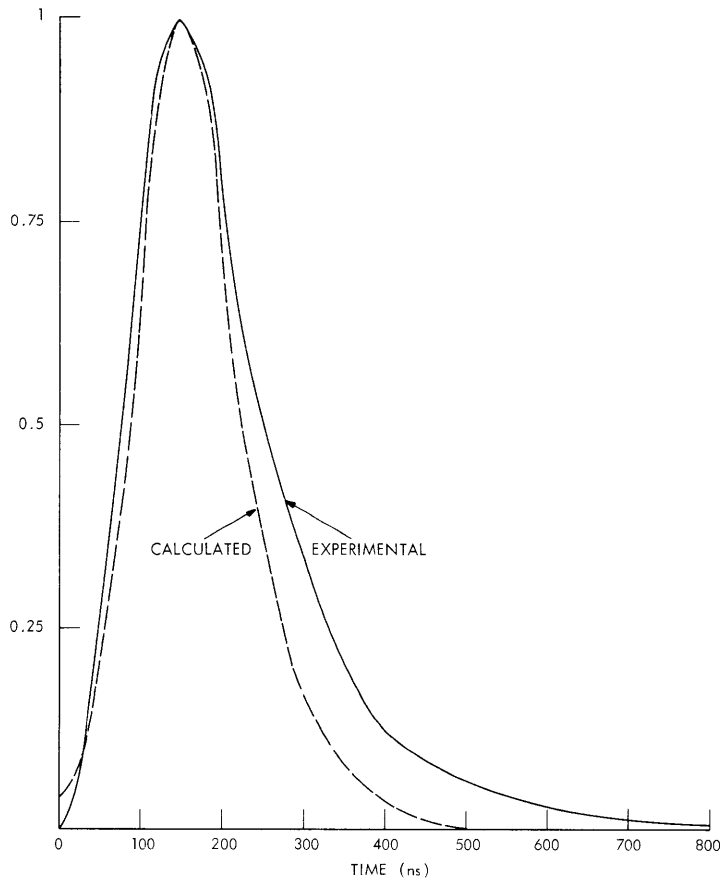

Fig. V-4. Normalized magnitude of detected optical signal.

both experimentally and analytically. An experimental value of 0.08 J compares well with the analytical prediction of .04 J/cm^2 (the plane-wave assumption necessitates leaving the detected signal in the form of power or energy per unit area). The confirmation of analysis by experiment is thus quite acceptable in terms of both the waveform of the optical pulse and its magnitude.

D. L. Lyon

References

1. A. J. Beaulieu, Appl. Phys. Letters 10, 504 (1970).
2. A. M. Robinson, Can. J. Phys. 48, 1996 (1970).
3. D. C. Smith and A. J. DeMaria, J. Appl. Phys. 41, 5212 (1970).
4. D. N. Duscik and E. Hoag, Avco Everett Research Laboratory Report (to be published).
5. C. Freed and A. Javan, Appl. Phys. Letters 17, 53 (1970).
6. W. L. Nighan, Report K-920833-5, United Aircraft Research Laboratories, Hartford, Connecticut, June 1971.
7. R. Dumanchin, Laser Focus 7, 32 (1971).
8. D. L. Lyon, E. V. George, and H. A. Haus, Appl. Phys. Letters 17, 474 (1970).
9. G. Herzberg, Infrared and Raman Spectra of Polyatomic Molecules (D. Van Nostrand Co., Inc., New York, 1945).
10. R. Sharma (to be published in J. Chem. Phys.).
11. A. I. Osipov and E. V. Stupochenko, Sov. Phys. – Usp. 6, 47 (1963).

B. GAIN AND RELAXATION STUDIES OF A TRANSVERSELY EXCITED ATMOSPHERIC (TEA) CO_2 LASER

1. Introduction

As a means of trying to understand some of the characteristics of and processes that occur in the TEA laser, it is useful to study it in an amplifier configuration, i.e., to study its response as an amplifier to an input cw low-intensity probe signal. The experiments that have been performed are TEA gain studies, and focus on two aspects of the gain: (i) the peak gain (and peak lengthwise averaged population inversion under certain assumptions) of a TEA amplifier as a function of total pressure, component gas partial pressure ratios, and several parameters which partially determine the amount of energy put into the amplifier; (ii) the decay of the gain vs time as a function of total pressure and component gas partial pressure ratios. This decay gives us insight into the relaxation of the upper laser level.

We have previously reported some preliminary measurements,[1] and we now report more conclusive results. Note that our model for the linear gain of a TEA amplifier is

$$\text{Gain} = G(t) = [I' + i(k)]/I = \exp(\alpha L),$$

where I and I' are the detector output currents with the amplifier empty and full, respectively, i(t) is the time-variant current following a pulsing of the amplifier with the zero (ac coupling) level assumed to be I', α is the gain coefficient (proportional to the inversion) and L is the length of the amplifier.

2. Peak Gain and Population Inversion

Determinations of the peak gain and population inversion have been made for various total pressures, partial pressure ratios, capacitances, and power supply voltages (small range).

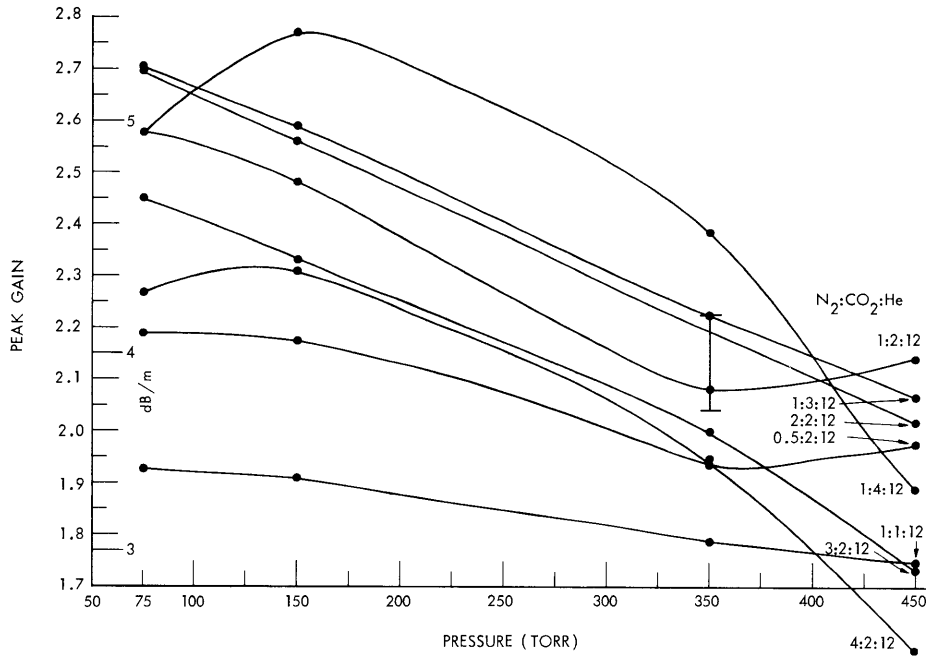

Fig. V-5. Peak gain vs pressure at 0.025 μF, 17.5 kV.

Figures V-5, V-6, and V-7 are plots of the peak gain vs pressure for various partial pressure ratios at a capacitance of 0.025 μF and power supply voltage of 17.5 kV. The discharge length is 83 cm. I and I' were determined for each point and the average of the maximum and minimum peaks for the six traces included in the single- and multiple-sweep pictures giving good views of i(t) are plotted. A plot of the range covered by the maximum and minimum at a ratio of 1:2:12, as shown in Fig. V-8, indicates a 5 to 15% variation. Even with the averaging, the variation is significant, as is indicated by the error bar on the 1:2:12, 350 Torr point in Fig. V-5. This covers the variation in the averaged peak gain (i.e., average of maximum and minimum) determined at various times during the period over which the data for these graphs were taken. This indicates that the results should be used mainly as an indicator of ranges and of trends (which are clear) with total pressure and partial pressure ratios. The partial pressure ratios are calculated from the flow rates with the partial pressure of each gas equaling its flow rate over the total flow rate of the 3 gases, multiplied

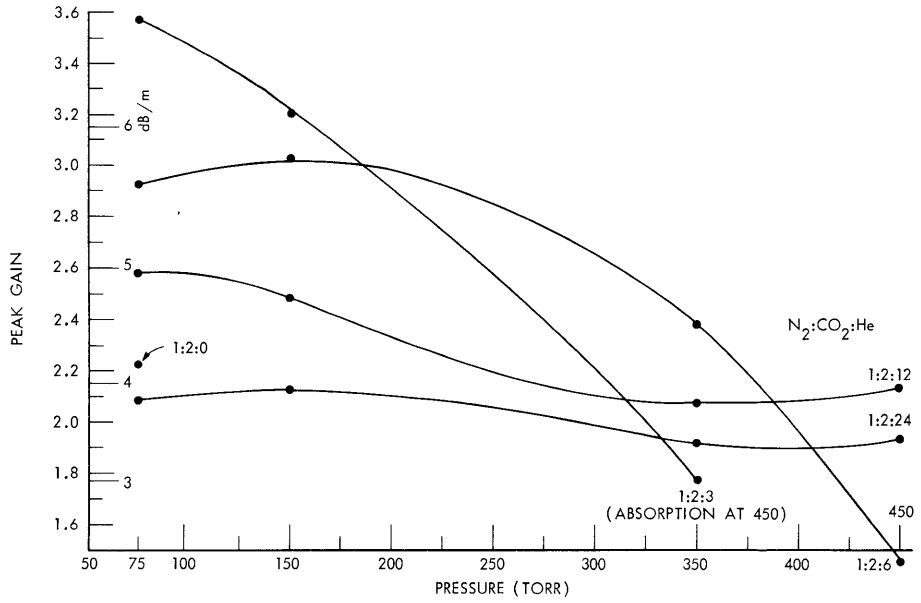

Fig. V-6. Peak gain vs pressure at 0.025 μF, 17.5 kV.

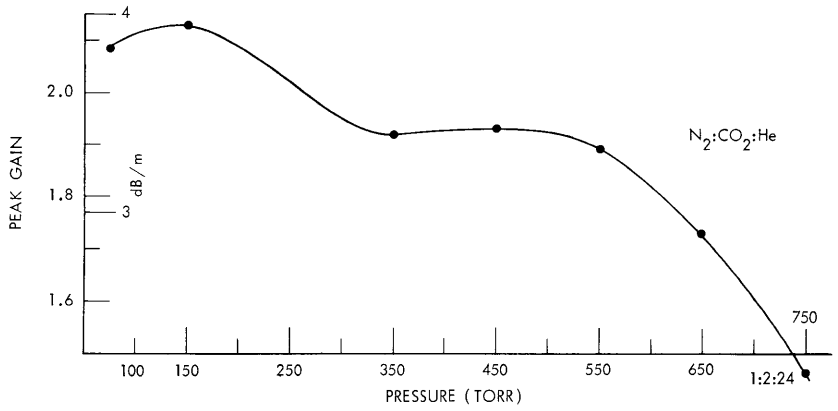

Fig. V-7.
Peak gain vs pressure at 0.025 μF, 17.5 kV.

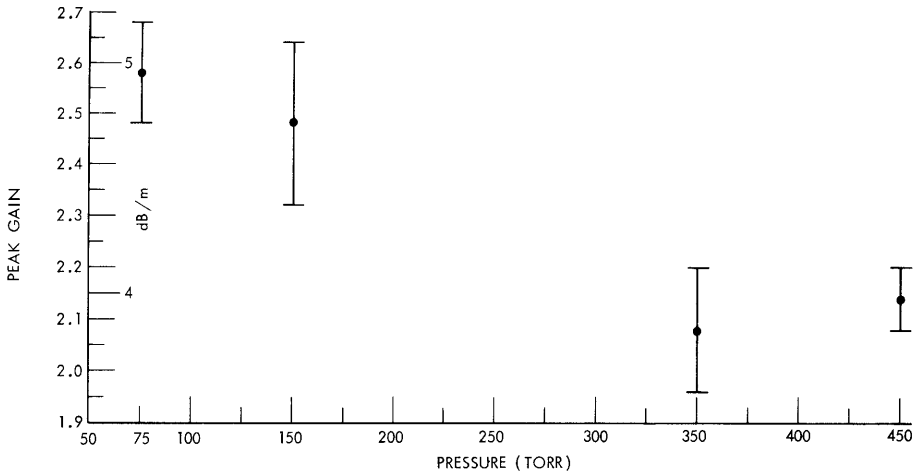

Fig. V-8.
Range of peak gain at 1:2:12, 0.025 μF, 17.5 kV.

by the total pressure in the amplifier.

The curves, first of all, indicate that with a couple of exceptions the gain increases with decreasing pressure. Also, increasing proportions of CO_2 result in increasing gain as long as the discharge is "good" – that is, at lower pressures. To the extent that CO_2 harms the discharge, increasing the CO_2 decreases the gain – i.e., at higher pressures. The curves tend to show that the optimal ratio of N_2 to CO_2 for the interaction between them involved in the inversion is near 1. This is concluded from the fact that among the 1:2:12, 2:2:12, 3:2:12, and 4:2:12 curves in which the partial pressures of He and CO_2 do not change a great deal (at a given total pressure), the 2:2:12 curve generally has the highest peak gain. Disregarding the 1:2:0 point, the gain vs increasing He partial pressure proportion (decreasing N_2 and CO_2 proportions) decreases at 75 Torr – a good discharge region. At 450 Torr, the opposite is true except for the 1:2:24 case. The low-pressure effect results from increasing proportions of CO_2 and N_2 in a good discharge region, and the higher pressure trend is because of the negative effects related to undesirable discharge characteristics. The 1:2:24 curve of Fig. V-7 indicates that for high He proportion mixes, a mid-pressure region may exist where discharge effects are stable.

Curves for the peak population inversion (rotational) calculated from the results of Figs. V-5, V-6, and V-7 are shown in Figs. V-9, V-10, and V-11. This inversion is calculated from the standard expression[1] for α using an assumed temperature of 300°K. The curves tend to be linear with pressure until bad discharge effects begin to dominate. On the other hand, the population inversion does not behave

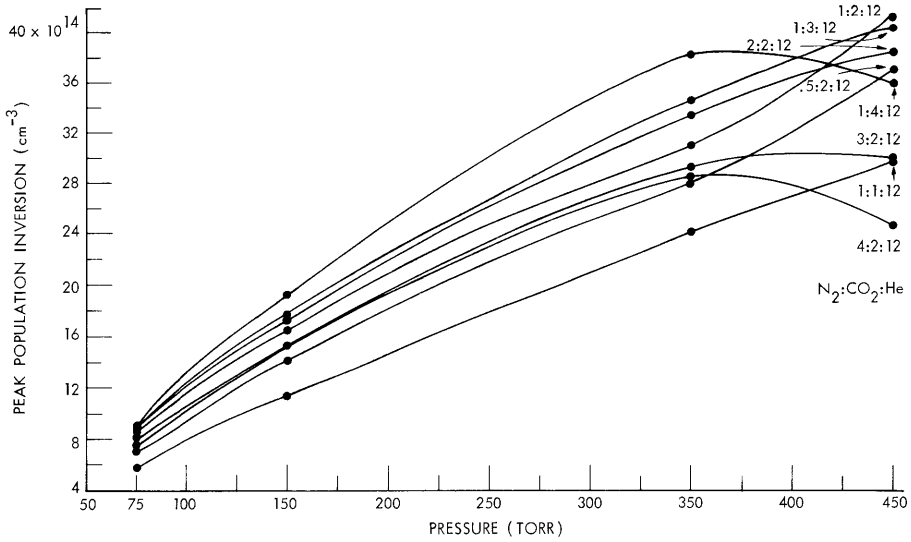

Fig. V-9. Peak population inversion vs pressure at 0.025 μF, 17.5 kV.

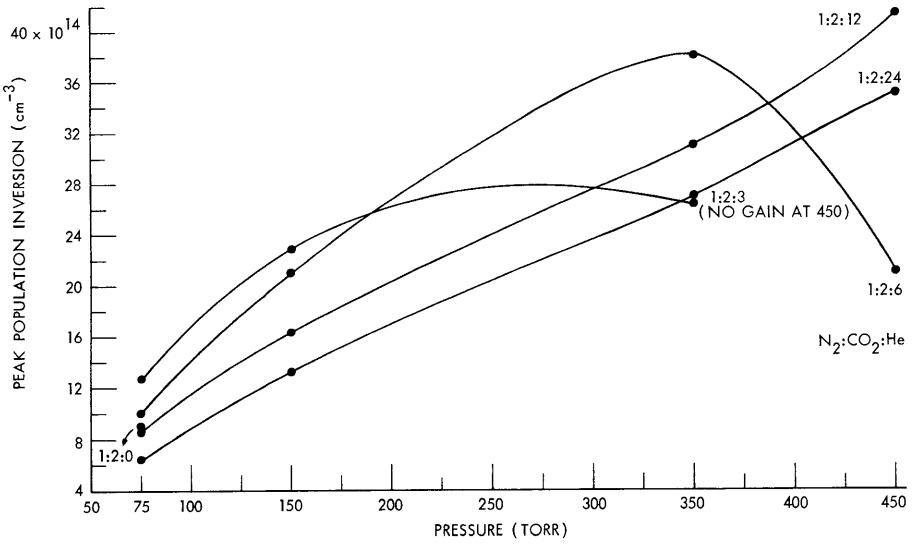

Fig. V-10. Peak population inversion vs pressure at 0.025 μF, 17.5 kV.

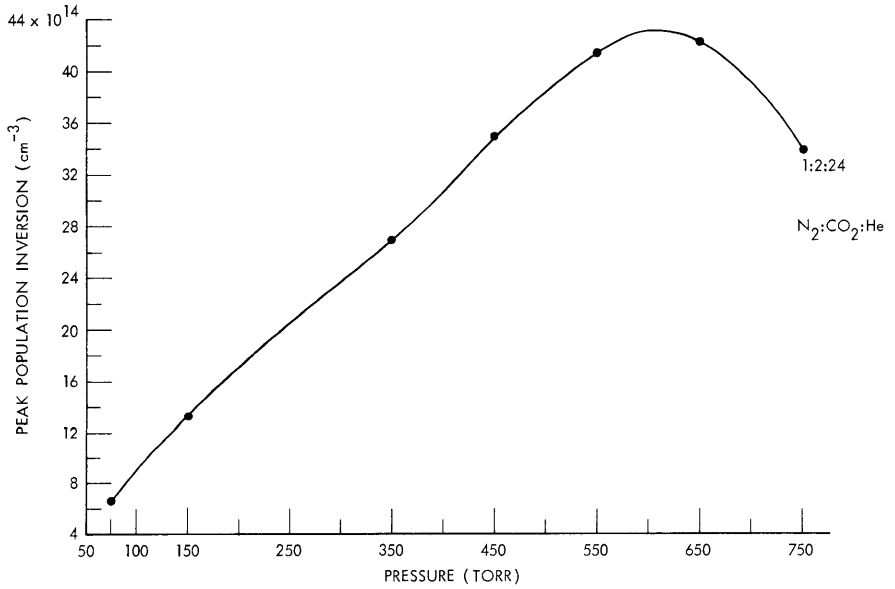

Fig. V-11. Peak population inversion vs pressure at 0.025 μF, 17.5 kV.

linearly with CO_2 partial pressure – see, for example, 1:1:12 and 1:2:12 between which the CO_2 pressure is approximately doubled and the N_2 and He pressures change very little. The fact that the nonlinearity is not less pronounced at low pressures indicates that it is not inherently related to discharge effects but probably stems from saturation of the energy available to create the inversion; that is, increasing the excitation circuit capacitance and power supply voltage should increase the gain.

Plots of the population inversion as a percentage of the CO_2 density, which are not included here, clearly show a decreasing percentage inversion with increasing CO_2, the existence of an optimal N_2:CO_2 ratio near 1, and discharge-related effects.

3. Upper Level Decay Rates

The decay of the upper laser level as a function of total pressure and partial pressure ratios may be studied from the single-sweep photograph giving good temporal discrimination of i(t) and the 10 ms/div i(t) photograph. This involves taking the ln (ln G(t)).

Table V-1 gives the experimentally determined decay times at various pressures and ratios; and Table V-2 gives the decay rates [1/(decay time)(total pressure)], which tend toward pressure independence. The average decay rate for each ratio has been calculated and is included. The result in parenthesis in Table V-1 for 1:2:12, 350 Torr is a second independently determined decay time for those conditions. It is obvious that N_2 decreases the decay rate and CO_2 increases it. The effect of He is not

Table V-1. Decay times (μs).

Ratios	Pressure (Torr)						
	75	150	350	450	550	650	750
1:2:24	238	116	53.2	37.6	36.4	30.0	26.8
1:2:12	220	110	39.2 (46.0)	32.8			
1:2:6	198	88.0	34.4	37.6			
1:2:3	128	61.0	25.6	—			
1:2:0	71	—	—	—			
1:1:12	312	156	74.0	56.0			
1:2:12	220	110	39.2	32.8			
1:3:12	192	101	46.0	27.6			
1:4:12	152	82	33.2	23.2			
5:2:12	192	86.0	50.4	32.8			
1:2:12	220	110	39.2	32.8			
2:2:12	252	132	50.8	47.2			
3:2:12	336	194	80.0	59.0			
4:2:12	460	200	95.0	64.0			
1:2:12 (18 kV, 0.0125 μF)	—	—	48.0	—			
1:2:12 (18 kV, 0.025 μF)	—	—	46.4	—			
1:2:12 (18 kV, 0.05 μF)	—	—	36.8	—			

Table V-2. Decay rates (s^{-1} $Torr^{-1}$).

Averages	Ratios	Pressure (Torr)						
		75	150	350	450	550	650	750
53.9	1:2:24	56.0	57.5	53.7	59.1	50.0	51.3	49.8
65.5	1:2:12	60.6	60.6	72.9	67.8			
71.3	1:2:6	67.3	75.8	83.1	59.1			
108	1:2:3	104	109	112	–			
188	1:2:0	188	–	–	–			
40.9	1:1:12	42.7	42.7	38.6	39.7			
65.5	1:2:12	60.6	60.6	72.9	67.8			
69.5	1:3:12	69.4	66.0	62.1	80.5			
87.7	1:4:12	87.7	81.3	86.1	95.8			
67.9	5:2:12	69.4	77.5	56.7	67.8			
65.5	1:2:12	60.6	60.6	72.9	67.8			
51.7	2:2:12	52.9	50.5	56.2	47.1			
36.9	3:2:12	39.7	34.4	35.7	37.7			
32.0	4:2:12	30.0	33.3	30.1	34.7			
59.5	1:2:12 (18 kV, 0.0125 μF)	–	–	59.5	–			
61.6	1:2:12 (18 kV, 0.025 μF)	–	–	61.6	–			
77.6	1:2:12 (18 kV, 0.05 μF)	–	–	77.6	–			

immediately obvious. Using fluorescence data, we made a detailed comparison of these decay rates with theoretical rates (under perturbational assumptions).

4. Relaxation Rates

Theoretical studies in conjunction with fluorescence experiments have shown that collisional relaxation of vibrationally excited $CO_2^*(00^01)$ in the presence of N_2, assuming equilibrium between the $CO_2(00^0n_3)$ and $N_2(v)$ chains, and under the perturbational assumption that the ground vibrational level populations are unchanged despite the excitation and relaxation processes, may be expressed as[2]

$$\frac{1}{p\tau} = \frac{X_{CO_2}}{X_{CO_2} + \left(\frac{k_c}{k_c'}\right) X_{N_2}} \left[X_{CO_2} k_{CO_2\text{-}CO_2} + X_{N_2} \left(k_{CO_2\text{-}N_2} + \frac{k_c}{k_c'} k_{N_2\text{-}CO_2} \right) \right],$$

where $1/p\tau$ is the decay rate (s^{-1} $Torr^{-1}$) and de-excitation of vibrationally excited $N_2^*(1)$ by N_2 is ignored because of its slow rate. The X's represent mole fractions, or pressure fractions.

The factor $X_{CO_2} \Big/ \left[X_{CO_2} + (k_c/k_c')X_{N_2} \right]$ is the fraction of the $CO_2^*(00^01)$ and $N_2^*(1)$ excitation energy that resides in the $CO_2^*(00^01)$ level.

The extension of this equation to an N_2-CO_2-He system is straightforward:

$$\frac{1}{p\tau} = \frac{X_{CO_2}}{X_{CO_2} + \left(\frac{k_c}{k_c'}\right) X_{N_2}} \left[X_{CO_2} k_{CO_2\text{-}CO_2} + X_{N_2} \left(k_{CO_2\text{-}N_2} + \frac{k_c}{k_c'} k_{N_2\text{-}CO_2} \right) + X_{He} k_{CO_2\text{-}He} \right].$$

The k's as determined in fluorescence experiments are[3,4]

$$k_{CO_2\text{-}CO_2} = 330 \text{ Torr}^{-1} \text{ s}^{-1},$$

$$k_{CO_2\text{-}N_2} + \frac{k_c'}{k_c} k_{N_2\text{-}CO_2} = 110 \text{ s}^{-1} \text{ Torr}^{-1},$$

$$k_{CO_2\text{-}He} = 82 \text{ s}^{-1} \text{ Torr}^{-1}.$$

We have carried out room-temperature (300°K) calculations using the equations above

Table V-3. Experimental and theoretical decay rates (s^{-1} $Torr^{-1}$).

Difference (%)	Theoretical	Averages	Ratios	Pressure (Torr)						
				75	150	350	450	550	650	750
+17.6	65.4	53.9	1:2:24	56.0	57.5	53.7	59.1	50.0	51.3	49.8
+13.6	75.8	65.5	1:2:12	60.6	60.6	72.9	67.8			
+21.4	90.7	71.3	1:2:6	67.3	75.8	83.1	59.1			
+ 0.92	109	108	1:2:3	104	109	112	—			
-13.3	166	188	1:2:0	188	—	—	—			
+15.8	48.6	40.9	1:1:12	42.7	42.7	38.6	39.7			
+13.6	75.8	65.5	1:2:12	60.6	60.6	72.9	67.8			
+27.3	95.6	69.5	1:3:12	69.4	66.0	62.1	80.5			
+21.0	111	87.7	1:4:12	87.7	81.3	86.1	95.8			
+26.0	91.8	67.9	5:2:12	69.4	77.5	56.7	67.8			
+13.6	75.8	65.5	1:2:12	60.6	60.6	72.9	67.8			
+ 7.2	55.7	51.7	2:2:12	52.9	50.5	56.2	47.1			
+15.8	43.8	36.9	3:2:12	39.7	34.4	35.7	37.7			
+12.1	36.4	32.0	4:2:12	30.0	33.3	30.1	34.7			
+21.5	75.8	59.5	1:2:12 (18 kV, 0.0125 μF)	—	—	59.5	—			
+18.7	75.8	61.6	1:2:12 (18 kV, 0.025 μF)	—	—	61.6	—			
+23.8	75.8	77.6	1:2:12 (18 kV, 0.05 μF)	—	—	77.6	—			

and rates for the partial pressure ratios at which TEA upper laser level decay rates were determined. These perturbational "theoretical" results are compared with the experimental results in Table V-3. The percentage differences between the theoretical values and experimental average values are also given with

$$\% \text{ Difference} = \frac{\text{Theory} - \text{Average}}{\text{Theory}} \times 100.$$

The differences in themselves are reasonable, given the perturbation assumptions made in the theoretical calculation, the uncertainties in the k's, and considering the assumptions made in the gain experiments. We would expect discrepancies related to the perturbation assumptions to be most severe in high CO_2 concentration cases as $k_{CO_2\text{-}CO_2}$ is by far the fastest.

If we ignore all the problems related to experimental assumptions and perturbation qualifications, temperature effects cannot explain the general slowness of the experimental results as gas heating increases the decay rates.[3,4] In fact, if we ignore the same factors, heating effects could make the 1:2:0 and 1:2:3 experimental results appear to be the most reasonable. This fact, along with the large percentage differences in the higher He proportion cases, might be interpreted as indicating that the efficiency of He in relaxing the upper laser level may not be as great in a discharge situation as in a fluorescence experiment in which $CO_2^*(00^01)$ is cleanly excited by 10.6 μm laser radiation. This possibility which first came to our attention in connection with low-pressure CO_2 laser gain experiments[5,6] cannot, however, be corroborated here because of the assumptions and qualifications of our experiment.

M. S. Elkind, P. W. Hoff

References

1. M. S. Elkind and P. W. Hoff, Quarterly Progress Report No. 102, Research Laboratory of Electronics, M.I.T., July 15, 1971, pp. 59-64.
2. C. B. Moore, R. E. Wood, B. L. Hu, and J. T. Yardley, "Vibrational Energy Transfer in CO_2 Lasers," J. Chem. Phys. 46, 4222-4231 (1967).
3. W. A. Rosser, Jr., A. D. Wood, and E. T. Gerry, "Deactivation of Vibrationally Excited Carbon Dioxide (ν_3) by Collisions with Carbon Dioxide or with Nitrogen*," J. Chem. Phys. 50, 4996-5008 (1969).
4. W. A. Rosser, Jr., and E. T. Gerry, "De-excitation of Vibrationally Excited $CO_2(\nu_3)$ by Collisions with He, O_2, H_2O," J. Chem. Phys. 51, 2286-2287 (1969).
5. P. K. Cheo, "Relaxation of CO_2 Laser Levels by Collisions with Foreign Gases," IEEE J. Quantum Electronics, Vol. QE-4, pp. 587-593, October 1968.
6. P. K. Cheo, "Effects of CO_2, He, and N_2 on the Lifetimes of the 00^01 and 10^00 Laser Levels and on Pulsed Gain at 10.6 μ," J. Appl. Phys. 38, 3563-3568 (1967).